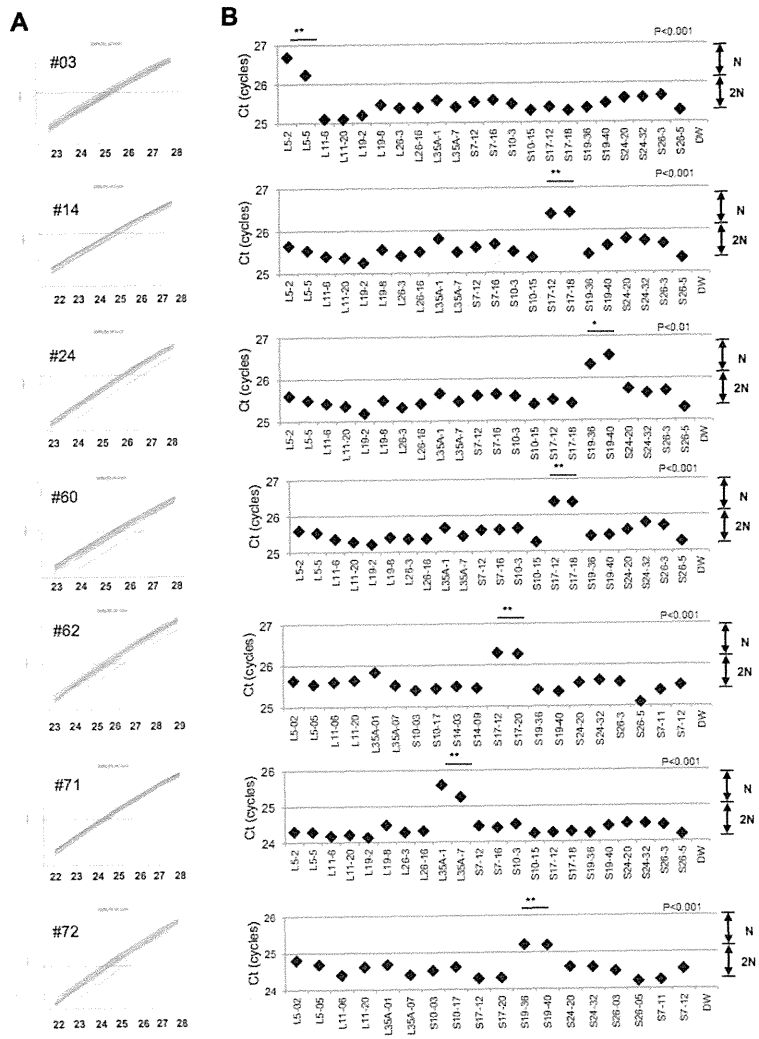

Figure 2. Detection of 7 mutations with a large deletion in DBA patients. Genomic DNA of 27 Japanese DBA patients with unknown mutations were subjected to the DBA gene copy number assay. (A) Amplification curve of s-q-PCR of a mutation with a large deletion. The deleted gene can be easily distinguished. (B) Ct score (cycles) of representative s-q-PCR with DBA genomic s-q-PCR primers. Results of the 2 gene-specific primer pairs indicated in the graph are representative of at least 2 sets for each gene-specific primer (carried out in the same run). $^{**}P < .001$; $^{*}P < .01$

chromosome 1 (ch1) spanning 858 kb (Figure 3A); patient 71 had a large deletion in ch3 spanning 786 kb (Figure 3B); patients 14, 60, and 62 had a large deletion in ch15 spanning 270 kb, 260 kb, and 330 kb, respectively (Figure 3C); and patient 72 had a large deletion in ch19 spanning 824 kb (Figure 3D). However, there were no deletions detected in ch19 in patient 24 (Figure 3D). Genes estimated to reside within a large deletion are listed in supplemental Table 1. Consistent with these s-q-PCR results, 6 of 7 large deletions were detected and confirmed as deleted regions, and these large deletions contained *RPL5*, *RPL35A*, *RPS17*, and *RPS19* (Table 4 and supplemental Table 1). Other large deletions in RP genes were not detected by this analysis. From these results, we conclude that the synchronized multiple PCR amplification method has a detection sensitivity comparable to that of SNP arrays.

Detailed examination of a patient with intragenic deletion in the RPS19 allele (patient 24)

Interestingly, for patient 24, in whom we could not detect a large deletion by SNP array at s-q-PCR gene copy number analysis, 2 primer sets for *RPS19* showed a 1-cycle delay (RPS19-36 and RPS19-40), but 2 other primer pairs (RPS19-58 and RPS19-62) did not show this delay (Figure 4A). We attempted to determine the deleted region in detail by testing more primer sets on *RPS19*. We tested a total of 9 primer sets for *RPS19* (Figure 4B) and examined the gene copy numbers. Surprisingly, 4 primer sets (S19-24, S19-36, S19-40, and S19-44) for intron 3 of *RPS19* indicated a 1-cycle delay, but the other primers for *RPS19* located on the 5′untranslated region (5′UTR), intron 3, or 3′UTR did not show this delay (S19-57, S19-58, S19-28, S19-62, and S19-65; Figure 4B-C). These results suggest that the intragenic deletion occurred in the *RPS19* allele. To confirm this deleted region precisely, we performed genomic PCR on *RPS19*, amplifying a region from the 5′UTR to intron 3 (Figure

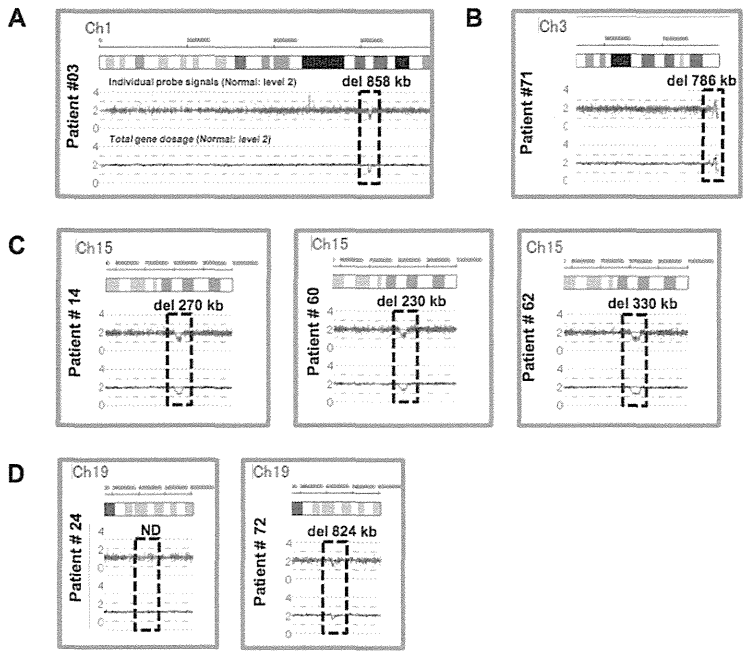

Figure 3. Results of SNP genomic microarray (SNP-chip) analysis. Genomic DNA of 27 Japanese DBA patients with unknown mutations was examined using a SNP array. Six patients had large deletions in their chromosome (ch), which included one DBA-responsible gene. Patient 3 has a large deletion in ch1 (A), patient 71 has a deletion in ch3 (B), patients 14, 60, and 62 have deletions in ch15 (C), and patient 72 has a deletion in ch19 (D).

4B). In patient 24, we observed an abnormally sized PCR product at a low molecular weight by agarose gel electrophoresis (Figure 4D). We did not detect a wild-type PCR product from the genomic PCR. This finding is probably because PCR tends to amplify smaller molecules more easily. However, we did detect a PCR fragment at the correct size using primers located in the supposedly deleted region. These bands were thought to be from the products of a wild-type allele. Sequencing of the mutant band revealed that intragenic recombination occurred at a homologous region of 27 nucleotides, from −1400 to −1374 in the 5′ region, to +5758 and +5784 in intron 3, which resulted in the loss of 7157 base pairs in the *RPS19* gene (Figure 4E). The deleted region contains exons 1, 2, and 3, and therefore the correct *RPS19* mRNA could not be transcribed.

Genotype-phenotype analysis and DBA mutations in Japan

Patients with a large deletion in DBA genes had common phenotypes (Table 4). Malformation with growth retardation (GR), including short stature or SGA, were observed in all 7 patients. In patients who had a mutation found by sequencing, half had GR (11 of 22; status data of DBA patients with mutations found by sequencing are not shown). GR may be a distinct phenotypic feature of large deletion mutations in Japanese DBA patients. Familial mutations were analyzed for parents for 5 DBA patients with a large deletion (patients 3, 24, 60, 62, and 72) by s-q-PCR. There are no large deletions in all 5 pairs of parents in DBA-responsible genes. Four of the 7 patients responded to steroid therapy. We have not observed significant phenotypic differences between patients with extensive deletions and other patients with regard to blood counts, responsiveness to treatment, or other malformations.

Discussion

Many studies have reported RP genes to be responsible for DBA. However, mutations have not been determined for approximately half of DBA patients analyzed. There are 2 possible reasons for this finding. One possibility is that patients have other genes responsible for DBA, and the other is that patients have a complicated set of mutations in RP genes that are difficult to detect. In the present study, we focused on the latter possibility because we have found fewer Japanese DBA patients with RP gene mutations (32.4%) compared with another cohort study of 117 DBA patients and 9 RP genes (approximately 52.9%).[4] With our newly developed method, we identified 7 new mutations with a large deletion in *RPL5*, *RPL35A*, *RPS17*, and *RPS19*.

The frequency of a large deletion was approximately 25.9% (7 of 27) in our group of patients who were not found to have mutations by genomic sequencing. Therefore, total RP gene mutations were confirmed in 42.6% of these Japanese patients (Table 5). Interestingly, mutations in *RPS17* have been observed at a high rate (5.9%) in Japan relative to that in other countries (1%).[5,15,16] Although the percentage of DBA mutations differs among different ethnic groups,[8,17-19] a certain portion of large deletions in DBA-responsible genes are likely to be determined in other countries by new strategies.

In the present study, we analyzed patient data to determine genotype-phenotype relations. To date, large deletions have been reported with RPS19 and RPL35A in DBA patients.[3,6,13] *RPS19* large deletions/translocations have been reported in 12 patients, and *RPL35A* large deletions have been reported in 2 patients.[19] GR in patients with a large deletion has been observed previously with *RPS19* translocations,[3,19-21] but it was not found in 2 patients with *RPL35A* deletion.[6] Interestingly, all of our patients with a large deletion had a phenotype

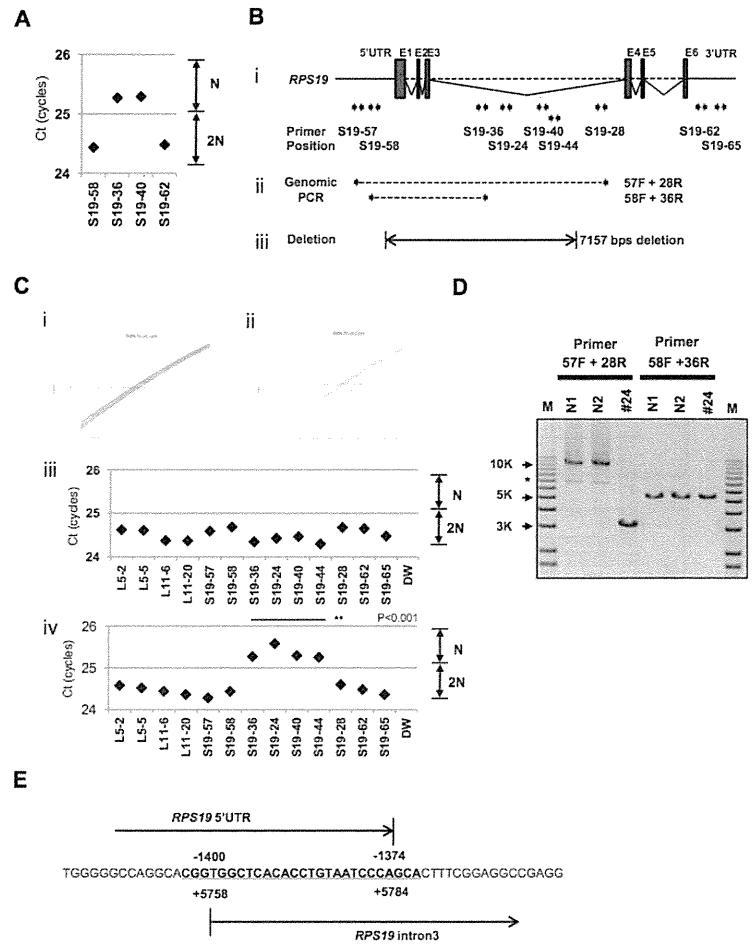

Figure 4. Result of s-q-PCR gene copy number assay for patient 24. (A) Results of s-q-PCR gene copy number assay for *RPS19* with 4 primer sets. (Bi) The *RPS19* gene copy number was analyzed with 9 specific primer sets for *RPS19* that span from the 5′UTR to the 3′UTR. (ii) Primer positions of genomic PCR for *RPS19*. (iii) Region determined to be an intragenic deletion in *RPS19*. (C) Results of gene copy number assay for *RPS19* show a healthy person (i,iii) and a DBA patient (ii,iv), and Ct results are shown (iii-iv). Patient 24 showed a "1-cycle delay" with primers located in the intron 3 region, but other primer sets were normal. (D) Results of genomic PCR amplification visualized by agarose gel electrophoresis to determine the region of deletion. N1 and N2 are healthy samples. *Nonspecific band. (E) Results from the genomic sequence of the 3-kb DNA band from genomic PCR on patient 24 showing an intragenic recombination from −1400 to 5784 (7157 nt) in *RPS19*. **$P < .001$.

of GR, including short stature and SGA, which suggests that this is a characteristic of DBA with a large gene deletion in Japan. Our study results suggest the possibility that GR is associated with extensive deletion in Japanese patients. Although further case studies will be needed to confirm this possibility, screening of DBA samples using our newly developed method will help to advance our understanding of the broader implications of the mutations and the correlation with the DBA genotype-phenotype.

Table 5. Total mutations in Japanese DBA patients, including large gene deletions

Gene	Mutation rate
RPS19	12(17.6%)
RPL5	7(10.3%)
RPL11	3 (4.4%)
RPS17	4 (5.9%)
RPS10	1 (1.5%)
RPS26	1 (1.5%)
RPL35A	1 (1.5%)
RPS24	0
RPS14	0
Mutations, n (%)	29(42.6%)
Total analyzed, N	68

Copy number variation analysis of DBA has been performed by linkage analysis, and the *RPS19* gene was first identified as a DBA-susceptibility gene. Comparative genomic hybridization array technology has also been used to detect DBA mutations in *RPL35A*, and multiplex ligation-dependent probe amplification has been used for *RPS19* gene deletion analysis.[3,6,13,22] However, these analyzing systems have problems in mutation screening. Linkage analysis is not a convenient tool to screen for multiple genetic mutations, such as those in DBA, because it requires a high level of proficiency. Although comparative genomic hybridization technology is a powerful tool with which to analyze copy number comprehensively, this method requires highly specialized equipment and analyzing software, which limits accessibility for researchers. Whereas quantitative PCR–based methods for copy number variation analysis are commercially available (TaqMan), they require a standard curve for each primer set, which limits the number of genes that can be loaded on a PCR plate. To address this issue, a new method of analysis is needed. By stringent selection of PCR primers, the s-q-PCR method enables analysis of many DBA genes in 1 PCR plate and the ability to immediately distinguish a large deletion using the s-q-PCR amplification curve. In our study, 6 of 7 large deletions in the RP gene detected by s-q-PCR were confirmed by SNP arrays (Figure 3). Interestingly, we detected

1 large intragenic deletion in *RPS19*, which was not detected by the SNP array. This agreement between detection results suggests that the s-q-PCR copy number assay could be useful for detecting large RP gene deletions.

In the present study, 7 DBA patients carried a large deletion in the RP genes. This type of mutation could be underrepresented by sequencing analysis, although in the future, genome sequencing might provide a universal platform for mutation and deletion detection. We propose that gene copy number analysis for known DBA genes, in addition to direct sequencing, should be performed to search for a novel responsible gene for DBA. Although at present, it may be difficult to observe copy numbers on all 80 ribosomal protein genes in one s-q-PCR assay, our method allows execution of gene copy number assays for several target genes in 1 plate. Because our method is quick, easy, and low cost, it could become a conventional tool for detecting DBA mutations.

Acknowledgments

The authors thank Momoka Tsuruhara, Kumiko Araki, and Keiko Furuhata for their expert assistance.

This work was partially supported by grants-in-aid for scientific research from the Ministry of Education, Culture, Sports, Science and Technology of Japan, and by Health and Labor Sciences research grants (Research on Intractable Diseases) from the Ministry of Health, Labor and Welfare of Japan.

Authorship

Contribution: M.K. designed and performed the research, analyzed the data, and wrote the manuscript; A.S-O. and S. Ogawa performed the SNP array analysis; T.M., M.T., and M.O designed the study; T.T, K. Terui, and R.W. analyzed the mutations and status data; H.K., S. Ohga, A.O., S.K., T.K., K.G., K.K., T.M., and N.M. analyzed the status data; A.M., H.M., K. Takizawa, T.M., and K.Y., performed the research and analyzed the data; E.I. and I.H. designed the study and analyzed the data; and all authors wrote the manuscript.

Conflict-of-interest disclosure: The authors declare no competing financial interests.

Correspondence: Isao Hamaguchi, MD, PhD, Department of Safety Research on Blood and Biological Products, National Institute of Infectious Diseases, 4-7-1, Gakuen, Musashimurayama, Tokyo 208-0011, Japan; e-mail: 130hama@nih.go.jp; or Etsuro Ito, MD, PhD, Department of Pediatrics, Hirosaki University Graduate School of Medicine, 5 Zaifucho, Hirosaki, Aomori 036-8562, Japan; e-mail: eturou@cc.hirosaki-u.ac.jp.

References

1. Hamaguchi I, Flygare J, Nishiura H, et al. Proliferation deficiency of multipotent hematopoietic progenitors in ribosomal protein S19 (RPS19)-deficient diamond-Blackfan anemia improves following RPS19 gene transfer. *Mol Ther.* 2003;7(5 pt 1):613-622.
2. Vlachos A, Ball S, Dahl N, et al. Diagnosing and treating Diamond Blackfan anaemia: results of an international clinical consensus conference. *Br J Haematol.* 2008;142(6):859-876.
3. Draptchinskaia N, Gustavsson P, Andersson B, et al. The gene encoding ribosomal protein S19 is mutated in Diamond-Blackfan anaemia. *Nat Genet.* 1999;21(2):169-175.
4. Doherty L, Sheen MR, Vlachos A, et al. Ribosomal protein genes RPS10 and RPS26 are commonly mutated in Diamond-Blackfan anemia. *Am J Hum Genet.* 2010;86(2):222-228.
5. Gazda HT, Sheen MR, Vlachos A, et al. Ribosomal protein L5 and L11 mutations are associated with cleft palate and abnormal thumbs in Diamond-Blackfan anemia patients. *Am J Hum Genet.* 2008;83(6):769-780.
6. Farrar JE, Nater M, Caywood E, et al. Abnormalities of the large ribosomal subunit protein, Rpl35a, in Diamond-Blackfan anemia. *Blood.* 2008;112(5):1582-1592.
7. Gazda HT, Grabowska A, Merida-Long LB, et al. Ribosomal protein S24 gene is mutated in Diamond-Blackfan anemia. *Am J Hum Genet.* 2006; 79(6):1110-1118.
8. Konno Y, Toki T, Tandai S, et al. Mutations in the ribosomal protein genes in Japanese patients with Diamond-Blackfan anemia. *Haematologica.* 2010;95(8):1293-1299.
9. Robledo S, Idol RA, Crimmins DL, Ladenson JH, Mason PJ, Bessler M. The role of human ribosomal proteins in the maturation of rRNA and ribosome production. *RNA.* 2008;14(9):1918-1929.
10. Léger-Silvestre I, Caffrey JM, Dawaliby R, et al. Specific Role for Yeast Homologs of the Diamond Blackfan Anemia-associated Rps19 Protein in Ribosome Synthesis. *J Biol Chem.* 2005;280(46): 38177-38185.
11. Choesmel V, Fribourg S, Aguissa-Toure AH, et al. Mutation of ribosomal protein RPS24 in Diamond-Blackfan anemia results in a ribosome biogenesis disorder. *Hum Mol Genet.* 2008;17(9):1253-1263.
12. Flygare J, Aspesi A, Bailey JC, et al. Human RPS19, the gene mutated in Diamond-Blackfan anemia, encodes a ribosomal protein required for the maturation of 40S ribosomal subunits. *Blood.* 2007;109(3):980-986.
13. Quarello P, Garelli E, Brusco A, et al. Multiplex ligation-dependent probe amplification enhances molecular diagnosis of Diamond-Blackfan anemia due to RPS19 deficiency. *Haematologica.* 2008; 93(11):1748-1750.
14. Yamamoto G, Nannya Y, Kato M, et al. Highly sensitive method for genomewide detection of allelic composition in nonpaired, primary tumor specimens by use of affymetrix single-nucleotide-polymorphism genotyping microarrays. *Am J Hum Genet.* 2007;81(1):114-126.
15. Song MJ, Yoo EH, Lee KO, et al. A novel initiation codon mutation in the ribosomal protein S17 gene (RPS17) in a patient with Diamond-Blackfan anemia. *Pediatr Blood Cancer.* 2010;54(4):629-631.
16. Cmejla R, Cmejlova J, Handrkova H, Petrak J, Pospisilova D. Ribosomal protein S17 gene (RPS17) is mutated in Diamond-Blackfan anemia. *Hum Mutat.* 2007;28(12):1178-1182.
17. Cmejla R, Cmejlova J, Handrkova H, et al. Identification of mutations in the ribosomal protein L5 (RPL5) and ribosomal protein L11 (RPL11) genes in Czech patients with Diamond-Blackfan anemia. *Hum Mutat.* 2009;30(3):321-327.
18. Quarello P, Garelli E, Carando A, et al. Diamond-Blackfan anemia: genotype-phenotype correlations in Italian patients with RPL5 and RPL11 mutations. *Haematologica.* 2010;95(2):206-213.
19. Boria I, Garelli E, Gazda HT, et al. The ribosomal basis of Diamond-Blackfan Anemia: mutation and database update. *Hum Mutat.* 2010;31(12):1269-1279.
20. Campagnoli MF, Garelli E, Quarello P, et al. Molecular basis of Diamond-Blackfan anemia: new findings from the Italian registry and a review of the literature. *Haematologica.* 2004;89(4):480-489.
21. Willig TN, Draptchinskaia N, Dianzani I, et al. Mutations in ribosomal protein S19 gene and diamond blackfan anemia: wide variations in phenotypic expression. *Blood.* 1999;94(12):4294-4306.
22. Gustavsson P, Garelli E, Draptchinskaia N, et al. Identification of microdeletions spanning the Diamond-Blackfan anemia locus on 19q13 and evidence for genetic heterogeneity. *Am J Hum Genet.* 1998;63(5):1388-1395.

nature immunology

The earliest thymic T cell progenitors sustain B cell and myeloid lineage potential

Sidinh Luc[1–3], Tiago C Luis[1,10], Hanane Boukarabila[1,10], Iain C Macaulay[1], Natalija Buza-Vidas[1,4], Tiphaine Bouriez-Jones[1], Michael Lutteropp[1,3], Petter S Woll[1], Stephen J Loughran[1], Adam J Mead[1], Anne Hultquist[2], John Brown[3], Takuo Mizukami[1], Sahoko Matsuoka[1], Helen Ferry[1,9], Kristina Anderson[2], Sara Duarte[1], Deborah Atkinson[1], Shamit Soneji[3], Aniela Domanski[1], Alison Farley[4], Alejandra Sanjuan-Pla[4], Cintia Carella[5], Roger Patient[3], Marella de Bruijn[3], Tariq Enver[3,9], Claus Nerlov[4], Clare Blackburn[4], Isabelle Godin[6–8] & Sten Eirik W Jacobsen[1–3]

The stepwise commitment from hematopoietic stem cells in the bone marrow to T lymphocyte–restricted progenitors in the thymus represents a paradigm for understanding the requirement for distinct extrinsic cues during different stages of lineage restriction from multipotent to lineage-restricted progenitors. However, the commitment stage at which progenitors migrate from the bone marrow to the thymus remains unclear. Here we provide functional and molecular evidence at the single-cell level that the earliest progenitors in the neonatal thymus had combined granulocyte-monocyte, T lymphocyte and B lymphocyte lineage potential but not megakaryocyte-erythroid lineage potential. These potentials were identical to those of candidate thymus-seeding progenitors in the bone marrow, which were closely related at the molecular level. Our findings establish the distinct lineage-restriction stage at which the T cell lineage–commitment process transits from the bone marrow to the remote thymus.

At the heart of developmental and stem-cell biology, as well as regenerative medicine, is the fundamental process of lineage commitment from self-renewing multipotent stem cells to lineage-restricted progenitors. In all species and organ systems, this process occurs first during embryonic development but is recapitulated postnatally and in adult life by adult multipotent stem cells that replenish cell lineages with a limited lifespan. Hematopoiesis represents the mammalian paradigm of how multilineage diversity can be achieved through the commitment of multipotent stem cells to lineage-committed progenitors and the establishment of distinct blood cell lineages[1]. However, the exact cellular commitment pathways remain unclear[1,2].

Whereas lineage-restricted progenitors for all other blood cell lineages can be generated from self-renewing hematopoietic stem cells (HSCs) in the postnatal bone marrow, the final steps of restriction to the T lymphocyte lineage take place in the thymus[3]. Because the thymus cannot sustain HSCs, continuous thymopoiesis can be secured only through regular replenishment by bone marrow–resident thymus-seeding progenitors (TSPs)[4]. However, the commitment stage(s) at which these progenitors migrate from the bone marrow to the thymus is (are) unknown. The thymus contains multiple blood cell lineages[5,6], as does the bone marrow; however, the identification of multipotent progenitors in the thymus that match the lineage potential of candidate TSPs in the bone marrow has not been possible so far. Early thymic progenitors (ETPs) have been extensively studied in the adult thymus, but their exact lineage potentials and relationship to candidate TSPs in the bone marrow have remained unclear[7].

Studies evaluating the lineage potential of ETPs at the single-cell level have shown that a large fraction of ETPs from adult mice have combined T cell and myeloid (granulocyte-monocyte (GM)) potential[8,9]. B cell lineage potential, however, was not detected for single, highly purified ETPs from adult mice, which suggests that the most primitive progenitor in the thymus might have potential restricted to T cells and granulocytes-monocytes[8,9]. Similar studies of fetal thymus have supported the proposal that the potential of ETPs is restricted to T cells and granulocytes-monocytes and have failed to show any B cell potential[10,11]. However, other studies have reported even rarer ETPs from adult mice with combined T cell and B cell (but not myeloid) potential[6], and candidate TSPs identified in the bone marrow[7], such as common lymphoid progenitors (CLPs)[12], lymphoid-primed multipotent progenitors (LMPPs)[13] and HSCs[1], all have B cell potential. The megakaryocyte-erythroid (MkE) potential of ETPs is of particular relevance to the ongoing debate on whether

[1]Haematopoietic Stem Cell Laboratory, Weatherall Institute of Molecular Medicine, John Radcliffe Hospital, University of Oxford, Oxford, UK. [2]Hematopoietic Stem Cell Laboratory, Lund Stem Cell Center, Lund University, Lund, Sweden. [3]Medical Research Council Molecular Haematology Unit, Weatherall Institute of Molecular Medicine, University of Oxford, Oxford, UK. [4]Institute for Stem Cell Research, Medical Research Council Centre for Regenerative Medicine, University of Edinburgh, Edinburgh, UK. [5]European Molecular Biology Laboratory Mouse Biology Unit, Monterotondo, Italy. [6]Institut National de la Santé et de la Recherche Médicale U1009, Villejuif, France. [7]Institut Gustave Roussy, Villejuif, France. [8]University of Paris-Sud, Orsay, France. [9]Present addresses: Experimental Medicine Division, Nuffield Department of Clinical Medicine, John Radcliffe Hospital, Oxford, UK (H.F.) and University College London Cancer Institute, London, UK (T.E.). [10]These authors contributed equally to this work. Correspondence should be addressed to S.E.W.J. (sten.jacobsen@imm.ox.ac.uk).

Received 1 August 2011; accepted 1 February 2012; published online 19 February 2012; doi:10.1038/ni.2255

the first lineage-commitment step in hematopoiesis results in strict separation into common pathways for commitment to the myeloid and lymphoid lineage, as presented in the still-prevailing textbook hierarchical model of hematopoiesis[1,14], or whether early lymphoid progenitors sustain GM potential but not MkE potential[2,13,15], as reported in human studies as well[16,17]. The MkE potential of purified ETPs has yet to be investigated[5,6,8,9].

The fact that no multipotent thymic progenitors with the same lineage potentials as those of candidate multipotent TSPs in the bone marrow have been identified yet contributes to the considerable gap in understanding of the distinct roles of the local bone marrow and thymus environments in promoting distinct prethymic and thymic stages of commitment to the T cell lineage. Here we demonstrate at the single-cell level the existence of postnatal ETPs with combined T cell, GM and B cell potential but no MkE potential, establishing the exact lineage commitment step at which the multipotent T lymphocyte progenitors must migrate to the thymus to allow the final steps of restriction to the T cell lineage to be completed. The data reported here provide further support for a myeloid-based model of commitment of hematopoietic-lineage cells to the T cell lineage.

RESULTS

ETPs have combined T cell, B cell and GM potential

The present knowledge about candidate TSPs and ETPs can be reconciled (**Supplementary Fig. 1**) only if a progenitor restricted to the T cell–GM lineage can be identified in the bone marrow, a T cell–GM

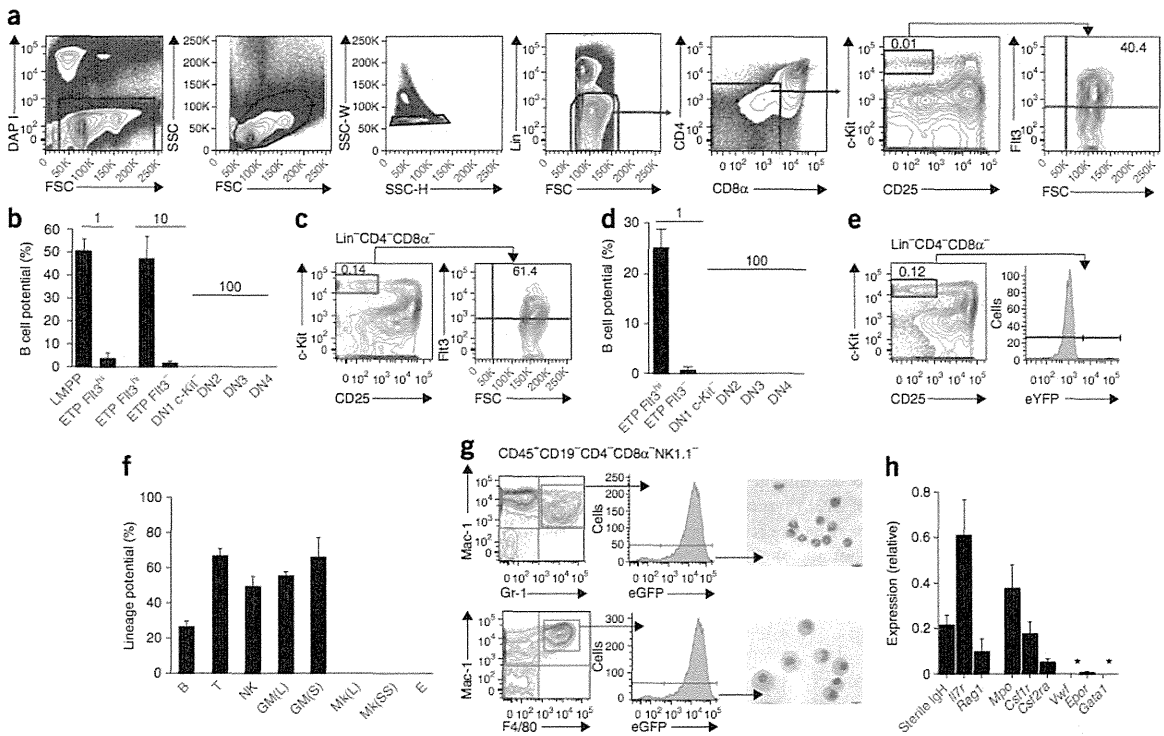

Figure 1 ETPs are multipotent lympho-myeloid restricted progenitors. (**a**) Flow cytometry profiles and gating strategies for the detection of Lin$^-$CD4$^-$CD8α$^-$CD25$^-$c-Kit^{hi}Flt3^{hi} ETPs from young adult mice (4–6 weeks). Numbers in plots indicate percent ETPs among total thymocytes. DAPI, *DNA-intercalating dye*; FSC, *forward scatter*; SSC, *side scatter*; -W, *width*; -H, *height*. (**b**) *Frequency of* B cell potential of cultures seeded with a single Lin$^-$Sca-1$^+$c-Kit$^+$Flt3^{hi} bone marrow cell (LMPP; $n = 320$); a single Flt3^{hi} ETP ($n = 73$ cells) or ten Flt3^{hi} ETPs ($n = 960$ cells); ten Flt3$^-$ ETPs ($n = 960$ cells); or other DN thymocyte progenitor populations (DN1–DN4; $n = 2{,}400$ cells (seeded with 100 cells per well)), all from adult mice. (**c**) Flow cytometry profiles and gating strategies as in **a**, for cells from newborn mice (1 d). (**d**) Frequency of B cell potential as in **b**, for cultures of cells from newborn mice, seeded as single Flt3^{hi} ETPs ($n = 348$ cells) or single Flt3$^-$ ETPs ($n = 210$ cells), and other DN thymocyte progenitor populations seeded at 100 cells per culture ($n = 4{,}200$–$6{,}000$ cells). (**e**) Expression of enhanced yellow fluorescent protein (eYFP) in ETPs from neonatal mice ($n = 4$) expressing Cre from the *Cd79a* promoter. (**f**) Frequency of cells with B cell potential (B; $n = 348$ cells), T cell potential (T; $n = 204$ cells), natural killer cell potential (NK; $n = 48$ cells), GM potential (grown in liquid (GM(L); $n = 600$ cells) or on stroma (GM(S); $n = 64$ cells)), megakaryocyte potential (grown in liquid (Mk(L); $n = 1{,}080$ cells) or on semisolid support (Mk(SS); $n = 6$; 200 cells per replicate)) or erythroid potential (E; $n = 8$; 500–1,000 cells per replicate) among Flt3$^+$ ETPs from neonatal mice (positive controls, **Supplementary Fig. 5**). (**g**) Expression of myeloid markers Mac-1, Gr-1 and lysozyme M (reported as eGFP expression; left and middle), and morphological analysis (right) of sorted granulocytes (top) and monocytes (bottom) from cultured Flt3$^+$ ETPs from neonatal mice. Scale bars, 5 μM. (**h**) Quantitative analysis of the expression of genes associated with lymphoid cells, myeloid cells and megakaryocytes–erythroid cells by purified Flt3$^+$ ETPs from newborn mice ($n = 6$; 25 cells per replicate); results are presented relative to the expression of *Hprt* (*encoding hypoxanthine guanine phosphoribosyl transferase*). *, ≤0.001 (*below detection limit*). Data are representative of four experiments (**a**); fourteen experiments (**c**); seven (**b**) or sixteen (**d**) experiments (Flt3^{hi} ETPs); sixteen experiments (bone marrow; **b**); four experiments (Flt3$^-$ ETPs (**b**) and other DN populations (**b**,**d**)); ten experiments (Flt3$^-$ ETPs; **d**); one experiment (**e**); two to sixteen experiments (**f**); one experiment (**g**); or two experiments (**h**; mean and s.e.m. in **b**,**d**,**f**; average and s.d. of six replicates in **h**).

progenitor can be generated in the passage from the bone marrow to the thymus and/or a thymic cell population with combined T cell, GM and B cell lineage potential can be identified among or beyond the ETPs. In the last scenario, the ETP could either be a lymphoid-GM–restricted multipotent progenitor or a pluripotent hematopoietic stem cell or progenitor cell that also has MkE potential. ETPs have been studied mostly in adult mice[5,6,8,9]. However, thymic involution (the physiological shrinking of the thymus with age that occurs in all vertebrates) indicates that thymopoiesis, and therefore thymus seeding, is much more active in the early postnatal thymus[18]. The B cell potential of early thymocytes, at the population level, is much higher (although still low) in the neonatal thymus than in the adult thymus[19]. In agreement with published studies, lineage-negative (Lin^-) $CD4^-CD8\alpha^-CD25^-c\text{-}Kit^{hi}$ ETPs represented only 0.01% of adult thymocytes[5], but as many as 40% of ETPs had cell-surface expression of the cytokine tyrosine kinase receptor Flt3, a greater frequency than reported before[20] (**Fig. 1a**). Also in agreement with published findings[6,20], a low but highly reproducible frequency of Flt3-expressing ETPs from adult mice generated B cells (3.5%–4.5%), whereas no other thymocyte progenitors from adult mice, including $Flt3^-$ ETPs, had any detectable B cell potential (**Fig. 1b** and **Supplementary Fig. 2**). The frequency of $Lin^-CD4^-CD8\alpha^-CD25^-c\text{-}Kit^{hi}Flt3^{hi}$ ETPs was more than tenfold higher in newborn mice than in adult mice (**Fig. 1c**) and, most notably, the frequency of $Lin^-CD4^-CD8\alpha^-CD25^-c\text{-}Kit^{hi}Flt3^{hi}$ ETPs with B cell potential was 25% (**Fig. 1d** and **Supplementary Fig. 3**). Neither $Lin^-CD4^-CD8\alpha^-CD25^-c\text{-}Kit^{hi}Flt3^-$ thymocytes nor downstream populations at $CD4^-CD8^-$ double-negative stages 2–4 (DN2–DN4) in the neonatal thymus had any B cell potential (**Fig. 1d**). $Lin^-CD4^-CD8\alpha^-CD25^-c\text{-}Kit^{hi}Flt3^{hi}$ ETPs from newborn mice also produced B cells *in vivo* when transplanted into irradiated mice deficient in recombination-activating gene 1 ($Rag1^{-/-}$) but produced only very low numbers of short-lived myeloid cells (**Supplementary Fig. 4**).

Because B cell activity in the thymus might reflect the presence of cells already committed to the B cell lineage[21,22], which overlap with the $CD25^-CD44^+$ phenotype of DN1 thymocytes, we did a fate-mapping experiment with mice expressing Cre recombinase from the promoter of the gene encoding the immunoglobulin-associated antigen CD79A (*Cd79a*), in which all committed B cell progenitors and their progeny are labeled with enhanced yellow fluorescent protein[23,24]. In agreement with published studies[23], cells of the B cell lineage, including all $CD19^+B220^+CD43^+c\text{-}Kit^+$ pro-B cells, as well as a fraction of $Ly6D^+$ CLPs ($Lin^-CD19^-B220^-Sca\text{-}1^{lo}c\text{-}Kit^{lo}Flt3^+IL\text{-}7R\alpha^+Ly6D^+$), were labeled in the bone marrow (**Supplementary Fig. 5a,b**). We observed no cells expressing enhanced yellow fluorescent protein among $Lin^-CD4^-CD8\alpha^-CD25^-c\text{-}Kit^{hi}$ ETPs (**Fig. 1e**) or among $Ly6D^-$ CLPs ($Lin^-CD19^-B220^-Sca\text{-}1^{lo}c\text{-}Kit^{lo}Flt3^+IL\text{-}7R\alpha^+Ly6D^-$) or LMPPs ($Lin^-Sca\text{-}1^+c\text{-}Kit^{hi}Flt3^{hi}$; **Supplementary Fig. 5b,c**).

In addition to producing B cells, $Lin^-CD4^-CD8\alpha^-CD25^-c\text{-}Kit^{hi}Flt3^{hi}$ ETPs from newborn mice gave rise efficiently to cells of the T cell, natural killer cell and GM lineages, as demonstrated before with ETPs from adult mice[5,6,8,9] (**Fig. 1f,g** and **Supplementary Fig. 6a**). In contrast, ETPs from newborn mice were completely devoid of MkE potential (**Fig. 1f**). ETPs from adult mice lacked megakaryocyte potential as well but, in agreement with published studies[8,9], had GM potential (**Supplementary Fig. 6a**). Quantitative gene-expression analysis showed that purified $Lin^-CD4^-CD8\alpha^-CD25^-c\text{-}Kit^{hi}Flt3^{hi}$ ETPs from newborn mice expressed many genes associated with granulocytes-monocytes and lymphoid cells but not those associated with megakaryocytes or erythroid cells (**Fig. 1h**). Single-cell PCR showed that as many as 65% of newborn $Lin^-CD4^-CD8\alpha^-CD25^-c\text{-}Kit^{hi}Flt3^{hi}$ ETPs coexpressed genes of granulocytes-monocytes and lymphoid cells, whereas they lacked expression of genes of megakaryocytes and erythroid cells (**Fig. 2a**).

To establish whether the T cell, B cell and GM potential of ETPs from neonatal mice reflected the existence of a multipotent lympho-myeloid progenitor in the thymus or only a mixture of lineage-restricted progenitors, we assessed the combined lineage potential of single $Lin^-CD4^-CD8\alpha^-CD25^-c\text{-}Kit^{hi}Flt3^{hi}$ ETPs. We sorted single ETPs onto OP9 bone marrow stroma to allow each single ETP to proliferate for 54 h, after which we split the expanded cell cultures and transferred them for an additional week to OP9 stroma and OP9 stroma expressing the Notch ligand Delta-like 1 (OP9-DL1 stroma) to promote differentiation into B cells and combined differentiation into T cells and myeloid cells, respectively.

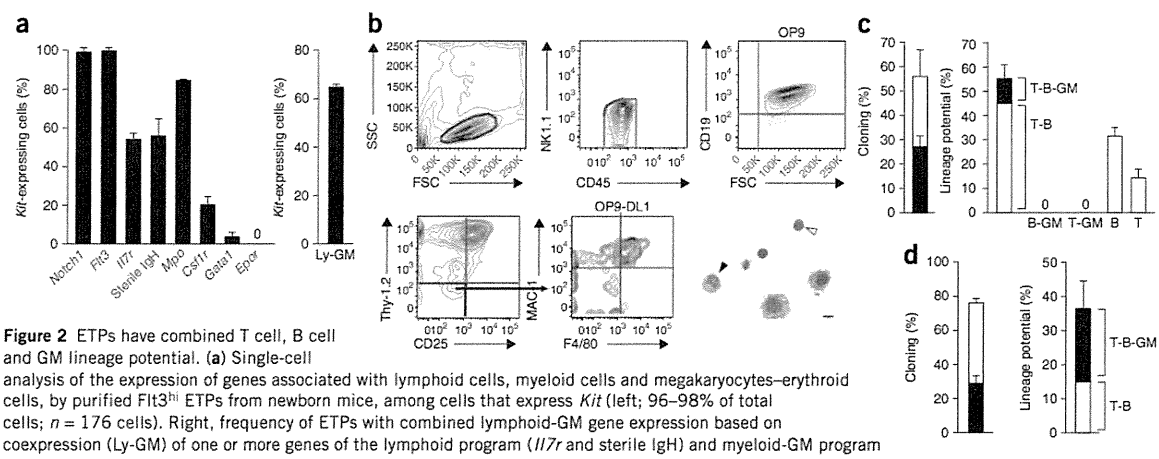

Figure 2 ETPs have combined T cell, B cell and GM lineage potential. (**a**) Single-cell analysis of the expression of genes associated with lymphoid cells, myeloid cells and megakaryocytes–erythroid cells, by purified $Flt3^{hi}$ ETPs from newborn mice, among cells that express *Kit* (left; 96–98% of total cells; $n = 176$ cells). Right, frequency of ETPs with combined lymphoid-GM gene expression based on coexpression (Ly-GM) of one or more genes of the lymphoid program (*Il7r* and sterile IgH) and myeloid-GM program (*Csf1r* and *Mpo*) but not of the MkE program (*Gata1* and *Epor*). (**b**) Flow cytometry and morphology analysis of a clone from a single $Flt3^+$ETP cell from a newborn wild-type mouse, with combined T cell–B cell (white arrowhead) and myeloid (black arrowhead) lineage potential. Scale bar, 5 μm. (**c,d**) Cloning frequency (left) of ETPs generating $CD45^+$ cells (open bars) and $CD45^+$ cells that are also positive for T cell, B cell and/or GM markers (filled bars), assessed for wild-type mice (**c**) or vavP-*Mcl1*–trangenic mice (**d**). Right, lineage distribution of clones from single ETPs from wild-type mice (**c**; $n = 132$ cells) or vavP-*Mcl1*–trangenic mice (**d**; $n = 167$ cells). Data are from two experiments (**a,d**) or three experiments (**b,c**; mean and s.d. in **a** and mean and s.e.m. in **c,d**).

Although the frequency of ETP-derived clones with detectable GM potential was lower than that of assays in which only the GM differentiation of ETPs was promoted (**Fig. 1f**), we demonstrated the existence of single Lin$^-$CD4$^-$CD8α$^-$CD25$^-$c-Kit^{hi}Flt3^{hi} ETPs with combined T cell, B cell and GM lineage potential (9.2% of clones with a lineage 'readout'; **Fig. 2b,c** and **Supplementary Fig. 7a**). In fact, we tracked all the GM potential from wild-type ETPs to cells that not only had T cell potential, as demonstrated before[8,9], but also had B cell lineage potential (**Fig. 2c**). Next we used ETPs purified from mice expressing *Mcl1* (encoding the antiapoptotic protein Mcl-1) from the vavP transgenic vector[25] to evaluate whether enhanced cell survival could better sustain short-lived myeloid cells in the assay for combined myeloid and T lymphoid development. Whereas the B cell potential in thymuses from neonatal *Mcl1*-transgenic mice remained restricted to Lin$^-$CD4$^-$CD8α$^-$CD25$^-$c-Kit^{hi}Flt3^{hi} ETPs (**Supplementary Fig. 7c**), the frequency of ETPs that generated combined T cell–B cell–GM progeny was 20% of all single ETPs (relative to 9.2% of wild-type ETPs) producing one or more hematpoietic lineages (**Fig. 2d** and **Supplementary Fig. 7b**). These findings obtained with single-cell clonal assays established the existence of thymic ETPs with combined T cell, B cell and GM lineage potential.

Lymphomyeloid ETPs are the most multipotent thymic progenitors

We next explored whether the Lin$^-$CD4$^-$CD8α$^-$CD25$^-$c-Kit^{hi}Flt3^{hi} ETPs with combined T cell, B cell and GM lineage potential represented the most multipotent progenitors in the neonatal thymus. The lack of detectable MkE potential in Lin$^-$CD4$^-$CD8α$^-$CD25$^-$c-Kit^{hi}Flt3^{hi} ETPs did not rule out the possibility of the presence of rare pluripotent hematopoietic stem cells or progenitor cells in the neonatal thymus. Thus, we first used highly sensitive flow cytometry to investigate the expression of three antigens, CD150 (ref. 26), CD201 (ref. 27) and Mpl[28]; each with high expression on most if not all HSCs as well as multipotent progenitors with sustained MkE potential. None of these antigens was expressed on Lin$^-$CD4$^-$CD8α$^-$CD25$^-$c-Kit^{hi} ETPs (**Fig. 3a**). Similar to a subfraction of bone marrow LMPPs, all ETPs expressed *Rag1*, as assessed through the use of a green fluorescent protein (GFP) reporter under control of the *Rag1* promoter[29], and most expressed the chemokine receptor CCR9 (**Fig. 3b**), in agreement with published studies of ETPs, LMPPs and CLPs from adult mice[30,31]. No bone marrow HSCs expressed either the *Rag1*-driven GFP reporter or CCR9 (**Fig. 3b**).

Whole thymocytes from neonatal mice transplanted intravenously or intrafemorally (to bypass potential changes in bone marrow–homing properties after entry into the thymus) into irradiated wild-type mice transiently reconstituted T cells and small amounts of B cells (**Fig. 3c,d**) but failed to sustain any long-term multilineage reconstitution (**Fig. 3e,f**), in further support of the idea that the postnatal thymus does not contain any HSCs. To enhance the detection of HSCs potentially present in the thymus, we depleted whole-thymocyte samples of CD4$^+$ and CD8$^+$ cells and transplanted these into recipient mice intravenously or intrafemorally (**Fig. 3g,h**). The absence of long-term

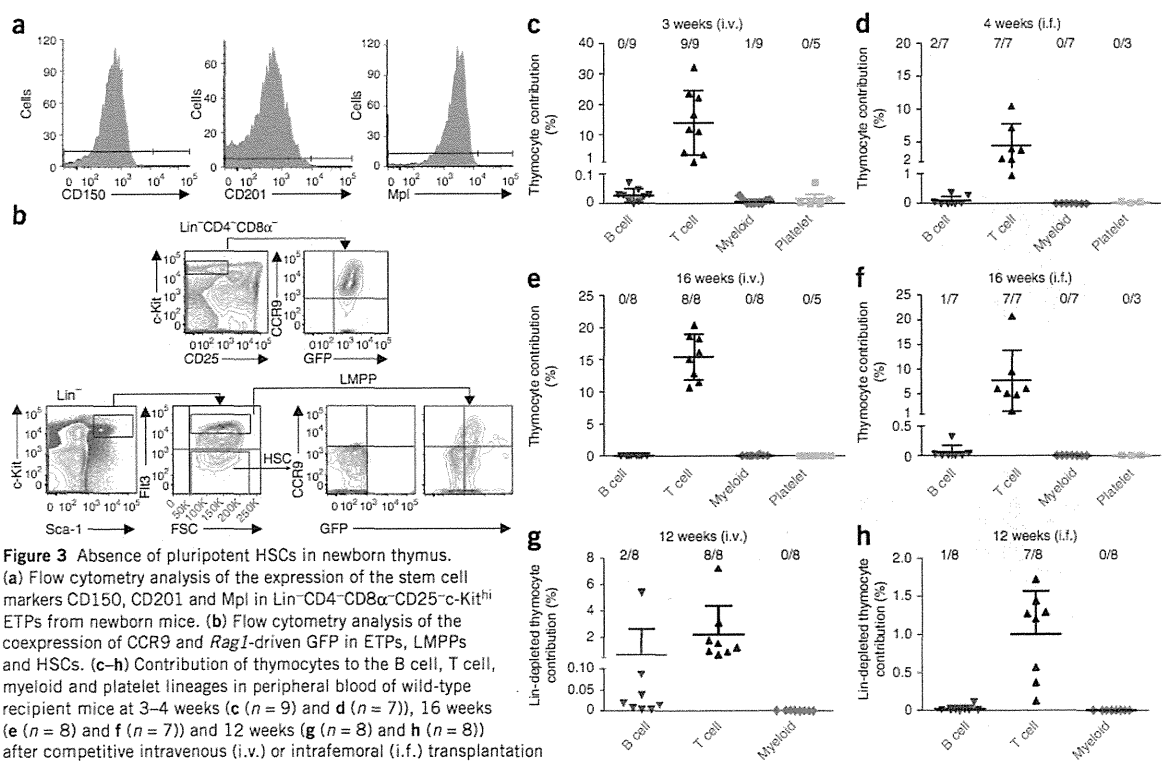

Figure 3 Absence of pluripotent HSCs in newborn thymus. (**a**) Flow cytometry analysis of the expression of the stem cell markers CD150, CD201 and Mpl in Lin$^-$CD4$^-$CD8α$^-$CD25$^-$c-Kit^{hi} ETPs from newborn mice. (**b**) Flow cytometry analysis of the coexpression of CCR9 and *Rag1*-driven GFP in ETPs, LMPPs and HSCs. (**c–h**) Contribution of thymocytes to the B cell, T cell, myeloid and platelet lineages in peripheral blood of wild-type recipient mice at 3–4 weeks (**c** ($n = 9$) and **d** ($n = 7$)), 16 weeks (**e** ($n = 8$) and **f** ($n = 7$)) and 12 weeks (**g** ($n = 8$) and **h** ($n = 8$)) after competitive intravenous (i.v.) or intrafemoral (i.f.) transplantation of total thymocytes (**c–f**) or of thymocyte samples depleted of CD4$^+$ and CD8$^+$ cells (Lin-depleted; **g,h**), from neonatal mice expressing eGFP driven by *Vwf* (in which all platelets express eGFP) or wild-type mice. Numbers at top indicate the frequency of reconstituted mice relative to total mice in group. Each symbol represents an individual mouse; horizontal lines indicate the mean (and s.d.). Data are representative of two experiments (**a,b**) or one experiment (**c–h**).

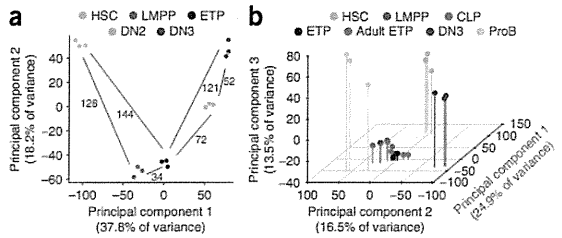

Figure 4 The gene expression of ETPs clusters closer to that of candidate TSPs in the bone marrow than to that of other thymic progenitors. Two- and three-dimensional principal-component analysis of normalized global gene-expression profiles of purified HSCs, IL-7Rα$^+$ LMPPs, ETPs, DN2 cells and DN3 cells from neonatal mice (**a**; $n = 3$ replicates), and purified HSCs ($n = 3$ replicates), IL-7Rα$^+$ LMPPs ($n = 3$ replicates), CLPs ($n = 4$ replicates), ETPs ($n = 3$ replicates), DN3 cells ($n = 3$ replicates) and pro-B cells ($n = 3$ replicates) from neonatal mice (**b**) and ETPs from adult mice (**b**; $n = 2$ replicates), with 1,600–2,000 cells per replicate. Each symbol represents an individual biological sample (sorted from a different pool of mice). Numbers adjacent to lines in **a** indicate Euclidean distances between average x and y values for each population measured in the first two principal components. Data are representative of three experiments (**a**) or two to three experiments (**b**).

myeloid reconstitution in all major hematopoietic organs, as well as the lack of thymocyte-derived T cell progenitors in the thymus after 13 weeks in all but one transplanted mouse, further confirmed the absence of pluripotent HSCs in the thymus (**Fig. 3g,h** and **Supplementary Fig. 8a–d**). Collectively, these results demonstrated the absence of HSCs in the postnatal thymus, a finding compatible with the proposal that ETPs with combined T cell, B cell and GM lineage potential are the most multipotent progenitors in the thymus.

ETPs are closely molecularly related to bone marrow TSPs

Because our findings indicated that Lin$^-$CD4$^-$CD8α$^-$CD25$^-$c-Kit^{hi}Flt3^{hi} ETPs in the neonatal thymus had the same lineage potential as Lin$^-$Sca-1$^+$c-Kit^{hi}Flt3^{hi} LMPPs expressing the *Rag1*-driven GFP reporter (which also had high expression of interleukin 7 receptor α (IL-7Rα); **Supplementary Fig. 9a**) in the bone marrow[13,32], we next investigated the molecular relationship between ETPs and IL-7Rα$^+$ LMPPs and HSCs in the bone marrow of neonatal mice. We also compared ETPs with the next stages of lineage restriction in the thymus: Lin$^-$CD44$^+$CD25$^+$c-Kit^{hi} DN2 cells, which sustain combined T cell and GM lineage potential but no B cell lineage potential[8,9], and Lin$^-$CD44$^-$CD25$^+$ DN3 cells, which represent the first T cell–restricted progenitors in the thymus[33]. Global gene-expression analysis done as described before[34], demonstrated that the gene-expression profile of ETPs clustered much closer to that of IL-7Rα$^+$ LMPPs in the bone marrow than to that of thymic DN2 or DN3 progenitors or bone marrow HSCs. Moreover, the gene-expression profile of LMPPs clustered closer to that of ETPs than to that of HSCs, and that of DN2 cells was closer to that of DN3 cells than to that of ETPs (**Fig. 4a**). Because CLPs have been suggested to be candidate TSPs[7] and have been shown to not only have lymphoid potential but also sustain some myeloid potential similar to LMPPs[35], we also compared the molecular profiles of ETPs with those of the two candidate TSP populations in the bone marrow: IL-7Rα$^+$ LMPPs and Lin$^-$CD19$^-$B220$^-$Sca-1^{lo}c-Kit^{lo}Flt3$^+$IL-7Rα$^+$Ly6D$^-$ CLPs[36] (**Fig. 4b**). The molecular profiles of ETPs from neonatal mice clustered closely with those of CLPs as well as those of LMPPs and were more distant from those of HSCs, DN3 cells and also pro-B cells. Moreover, the molecular profiles of ETPs from neonatal and adult mice clustered closely together with those of LMPPs and CLPs (**Fig. 4b**). These findings established a close molecular relationship between Lin$^-$CD4$^-$CD8α$^-$CD25$^-$c-Kit^{hi}Flt3^{hi} ETPs in

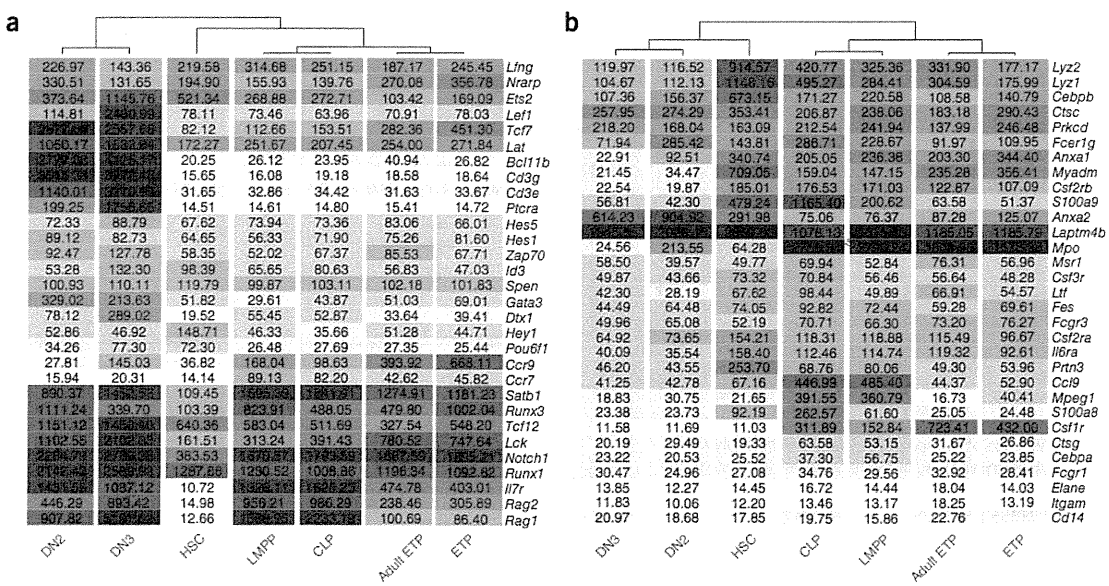

Figure 5 ETPs, IL-7Rα$^+$ LMPPs and CLPs have closely related T cell– and myeloid-lineage transcriptional profiles. Expression of genes associated with the T cell lineage (**a**) or GM lineage (**b**) by purified HSCs ($n = 6$ replicates), IL-7Rα$^+$ LMPPs ($n = 6$ replicates), CLPs ($n = 4$ replicates), ETPs ($n = 6$ replicates), DN2 cells ($n = 3$ replicates) and DN3 cells ($n = 6$ replicates) from neonatal mice, and ETPs from adult mice ($n = 2$ replicates), with 1,600–2,000 cells per replicate (derivation of gene lists, Online Methods and **Supplementary Note**). Numbers in boxes indicate normalized median values obtained by the robust multiarray average method: darker shading indicates higher expression; lighter shading indicates lower expression. Dendrograms above indicate relationships between samples according to their gene profiles. Data are representative of two to four experiments.

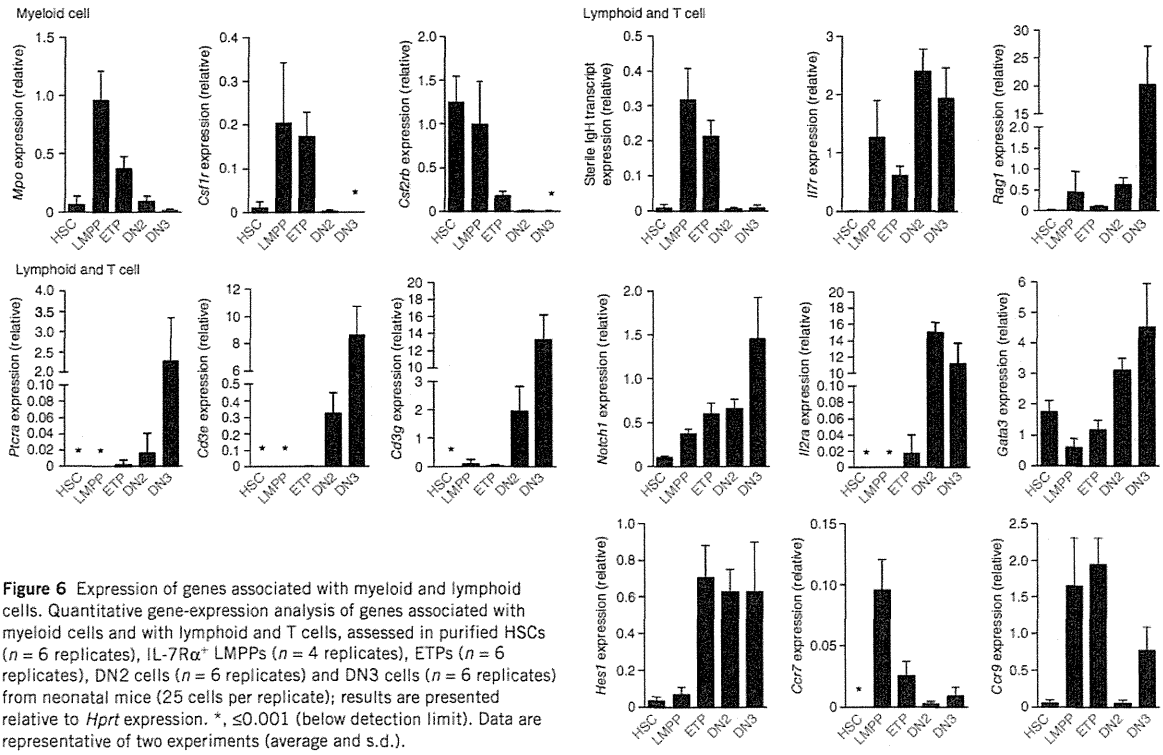

Figure 6 Expression of genes associated with myeloid and lymphoid cells. Quantitative gene-expression analysis of genes associated with myeloid cells and with lymphoid and T cells, assessed in purified HSCs ($n = 6$ replicates), IL-7Rα$^+$ LMPPs ($n = 4$ replicates), ETPs ($n = 6$ replicates), DN2 cells ($n = 6$ replicates) and DN3 cells ($n = 6$ replicates) from neonatal mice (25 cells per replicate); results are presented relative to *Hprt* expression. *, ≤0.001 (below detection limit). Data are representative of two experiments (average and s.d.).

the thymus and candidate TSPs with lympho-myeloid potential in the bone marrow (**Fig. 4a,b** and **Supplementary Fig. 9b,c**).

To more specifically assess gene expression associated with the T cell and GM lineages, we derived lists of genes associated with T cells and granulocytes-monocytes from the literature and from published data sets[37,38] (**Supplementary Note**). When we compared the programs associated with the T cell and GM lineages, we found that those of ETPs from adult and neonatal mice clustered closely for both the T cell and GM lineage, and closer to those for IL-7Rα$^+$ LMPPs and CLPs than to those for DN2 or DN3 cells in the thymus or HSCs in the bone marrow (**Fig. 5a,b** and **Supplementary Fig. 9d,e**). Notably, many T cell–associated genes that eventually undergo considerable upregulation in DN2 cells and even further after T cell commitment of DN3 cells, had already been upregulated in LMPPs and CLPs, relative to their low expression in HSCs. There was less change in expression of these T cell–associated genes in LMPPs and CLPs relative to their expression in ETPs (**Fig. 5a**). By quantitative RT-PCR, we investigated in greater detail some genes related to myeloid cells, lymphoid cells, T cells and Notch (**Fig. 6**). In addition to confirming the combined expression of genes associated with the GM lineage (*Mpo*, *Csf1r* and *Csf2rb*) and lymphoid lineage (sterile IgH, *Il7r* and *Rag1*) in ETPs and LMPPs, these data also showed that characteristic early T cell–specific genes (*Ptcra*, *Cd3e* and *Cd3g*) were not significantly upregulated in either multipotent IL-7Rα$^+$ LMPPs or ETPs. In contrast, *Notch1* was upregulated in LMPPs and even further upregulated in ETPs and, in agreement with that, the Notch target genes *Il2ra (Cd25)*, *Gata3* and, in particular, *Hes1* (ref. 39) were upregulated in the transition from LMPPs to ETPs. Finally, whereas HSCs lacked expression of *Ccr7* and *Ccr9*, which encode chemokine receptors critical for migration to the thymus[30,31], these genes showed considerable upregulation in IL-7Rα$^+$ LMPPs, in further support of the idea that LMPPs are TSPs. Collectively, these results demonstrated that ETPs and candidate TSPs such as LMPPs and CLPs had closely related gene-expression profiles, which reinforced the proposal that ETPs are more probably derived from lympho-myeloid–restricted TSPs than from HSCs in the bone marrow.

DISCUSSION

Here we have identified ETPs in the neonatal thymus with combined T cell, B cell and GM lineage potential but no MkE lineage potential, and we have demonstrated a close functional and molecular link between ETPs and candidate TSPs in the bone marrow. The observation that ETPs lacked MkE potential was notable for reconciliation of the ongoing debate about the roadmap for commitment to different hematopoietic lineages, as the classical model for such commitment indicates that the first lineage-commitment step of HSCs results in strict separation of the myeloerythroid- and lymphoid-commitment pathways[1,14]. According to that model, any cell with combined lymphoid and GM potential should also have MkE potential. However, we found that Lin$^-$CD4$^-$CD8α$^-$CD25$^-$c-Kit^{hi}Flt3^{hi} ETPs with combined T cell, B cell and GM lineage potential were devoid of megakaryocyte or erythroid lineage potential. These cells coexpressed, at the single-cell level, genes related to lymphoid cells and granulocytes-monocytes, but not megakaryocytes or erythroid cells, similar to LMPPs with identical lineage potentials in the bone marrow[13,32,34]. Thus, our study has provided further support for a myeloid-based lineage-commitment model[2,13,15–17] by demonstrating the existence of T cell–B cell–GM–restricted progenitors in the postnatal thymus. Such cells have been identified before in the bone marrow and fetal liver[13,34].

The real frequency of Lin$^-$CD4$^-$CD8α$^-$CD25$^-$c-Kit^{hi}Flt3^{hi} ETPs from neonatal mice with T cell–B cell–GM potential is probably higher than we were able to demonstrate. Analysis of clones grown from single ETPs from newborn mice demonstrated that most ETPs with T cell potential simultaneously had B cell potential, but less than 20% of these also showed GM potential in wild-type mice, although under optimized GM conditions more than 50% of ETPs demonstrated GM potential. We speculated that the lower detection of cells of the GM lineages in the multilineage clonal assay reflected the short lifespan of vulnerable myeloid cells, and in agreement with that, transgenic expression of the antiapoptotic protein Mcl-1 enhanced the generation of myeloid cells from ETPs with combined T cell, B cell and GM potential in neonatal mice, most probably through the enhanced survival of myeloid cells. Our findings also suggest that the T cell–B cell–GM restricted progenitor identified is the most multipotent progenitor in the neonatal thymus, as we did not detect any MkE lineage potential or MkE-specific gene expression among highly purified ETPs. Furthermore, we also demonstrated that there were no phenotypic or *in vivo* reconstituting HSCs or multipotent progenitors in the neonatal thymus.

Published studies have suggested that the earliest fetal thymic progenitors in the embryo have combined T cell and myeloid lineage potential but no B cell lineage potential[10,11], which raises the possibility that the progenitors that seed the embryonic thymus might be distinct from and more committed than those in the postnatal thymus. In contrast to the seeding of the neonatal thymus, which was the focus of our study, it remains unclear if the adult thymus is also seeded with ETPs with combined T cell, GM and B cell lineage potential. As thymopoiesis is much less active in adult thymus than in newborn thymus, it can be predicted that the most multipotent ETPs are much more infrequent in adult thymus than in the neonatal thymus. Although the low frequency of B cell lineage potential of ETPs from adult mice reported before[6,20] and confirmed here does not allow definitive demonstration of the combined T cell, GM and B cell lineage potentials of ETPs from adult mice with the present clonal lineage-potential assay, it is notable that rare Lin$^-$CD4$^-$CD8α$^-$CD25$^-$c-Kit^{hi}Flt3^{hi} ETPs were the only thymocytes from adult mice with B cell potential. In addition, we found that ETPs from adult mice, like ETPs from neonatal mice, had GM potential but not megakaryocyte potential, and global gene-expression analysis indicated a close molecular relationship between ETPs from neonatal mice and those from adult mice. Collectively, these data suggest that the adult thymus, like neonatal thymus, might also be seeded by rare T cell–B cell–GM progenitors, which we were unequivocally able to identify in neonatal thymus. Nevertheless, there are distinct differences among HSCs and hematopoietic progenitor cells from fetal, neonatal and adult mice. The regulated migration of TSPs to the thymus might also differ in the fetus, newborn and adult, so it remains possible that the lineage potentials of TSPs from embryos, newborns and adults might be different.

Although our studies have established the extent of ETP multipotentiality (T cell–B cell–GM) and the close phenotypic and molecular relationship of ETPs, LMPPs and CLPs with the same lineage potentials in the bone marrow[13,32,34,35], they do not exclude the possibility that other candidate progenitors in the bone marrow might seed the thymus[40]. A published study has suggested that T cell–GM–restricted progenitors might exist in the bone marrow[41], although such progenitors remain to be purified and characterized in further detail. The GM potential of ETPs is limited, and studies have suggested that it has little if any functional relevance to these progenitors' acting as myeloid progenitors in the thymus[35,42]. Likewise, it seems unlikely that ETPs have any important physiological role as B cell progenitors. Instead, the importance of these sustained lineage potentials of ETPs is to provide a better understanding of the lineage-restriction steps required for lineage commitment from pluripotent HSC in the bone marrow to a T cell–restricted progenitor in the thymus. Specifically, progenitors with combined T cell–B cell–GM potential, such as LMPPs and CLPs, are derived in the bone marrow from HSCs that have shut down the MkE transcriptional programs and lineage potential. Unlike HSCs, LMPPs and CLPs upregulate CCR9, which enables their transfer to the thymus[30,31]. Migration to the thymus seems critical for the next T cell lineage–restriction steps, first to a T cell–GM progenitor[8,9] and finally to a fully T cell–restricted progenitor.

Our studies have provided new insight into the normal stepwise process of commitment to the T cell lineage in the bone marrow and thymus. In addition, they are also relevant to the clinically, phenotypically and molecularly distinct group of mixed T cell–GM acute lymphoblastic leukemias that are mostly observed in children but also seen in adults, called 'ETP leukemias'[43]. Furthermore, the sustained B cell potential of ETPs might explain why the MLL-AF4 fusion oncogene that is highly specific for human B cell malignancies can give rise to B cell malignancies even if targeted to thymic progenitors[44].

METHODS

Methods and any associated references are available in the online version of the paper at http://www.nature.com/natureimmunology/.

Accession code. GEO: microarray data, GSE29382.

Note: Supplementary information is available on the Nature Immunology website.

ACKNOWLEDGMENTS

We thank N. Sakaguchi (Kumamoto University) for mice with *Rag1*-driven GFP expression; T. Graf (Center for Genomic Regulation) for mice with expression of enhanced GFP (eGFP) driven by the gene encoding lysozyme M[4]; S. Cory (Walter and Eliza Hall Institute of Medical Research) for vavP-*Mcl1*–trangenic mice; M. Reth (Max Planck Institute of Immunobiology) for Cd79a$^{tm1(cre)Reth}$ mice; S. Srinivas (University of Oxford) for mice expressing enhanced yellow fluorescent protein from the *Rosa26* locus; A. Cumano (Institut Pasteur) for OP9 and OP9-DL1 stromal cells; Biomedical Services at Oxford University for animal support; S. Clark, T. Furey and B. Wu for technical assistance; and E. Zuo and M. Eckart at the Stanford Protein and Nucleic Acid Facility for gene array services. Supported by the Medical Research Council, UK (H4RPLK0 to S.E.W.J. and EU-FP7 EuroSyStem Integrated projects to S.E.W.J., C.B. and A.F.), Leukaemia and Lymphoma Research (C.B., A.F. and A.J.M.), the Crafoord Foundation (A.H.), The George Danielsson Foundation (A.H.) and Swedish Society for Medicine and Swedish Cancer Foundation (A.H.).

AUTHOR CONTRIBUTIONS

S.E.W.J. and S.L. designed and conceived of the overall research, analyzed the data and wrote the manuscript, which was subsequently reviewed and approved by all authors; J.B. processed RNA samples; I.C.M. and S.S. analyzed the microarray data; A.J.M., D.A. and A.H. did quantitative and single-cell PCR; A.J.M., S.M. and K.A. did morphology analyses; H.F., S.L. and M.L. sorted cells by flow cytometry; S.L., M.L., T.B.-J., S.D., N.B.-V., H.B., T.C.L., A.D. and S.J.L. contributed to flow cytometry and *in vitro* culture experiments; S.L., S.D., N.B.-V., P.S.W., T.C.L. and H.B. did *in vivo* transplantations; T.E. provided assistance in the design and analysis of microarray experiments; C.B., A.F., R.P., M.d.B., I.G. and T.M. contributed advice and input on experimental design; and C.N., A.S.-P. and C.C. generated and provided input on studies of mice expressing eGFP driven by *Vwf* (encoding the von Willebrand factor homolog).

COMPETING FINANCIAL INTERESTS

The authors declare no competing financial interests.

Published online at http://www.nature.com/natureimmunology/.
Reprints and permissions information is available online at http://www.nature.com/reprints/index.html.

1. Reya, T., Morrison, S.J., Clarke, M.F. & Weissman, I.L. Stem cells, cancer, and cancer stem cells. *Nature* **414**, 105–111 (2001).
2. Katsura, Y. Redefinition of lymphoid progenitors. *Nat. Rev. Immunol.* **2**, 127–132 (2002).
3. Donskoy, E. & Goldschneider, I. Thymocytopoiesis is maintained by blood-borne precursors throughout postnatal life. A study in parabiotic mice. *J. Immunol.* **148**, 1604–1612 (1992).
4. Scollay, R., Smith, J. & Stauffer, V. Dynamics of early T cells: prothymocyte migration and proliferation in the adult mouse thymus. *Immunol. Rev.* **91**, 129–157 (1986).
5. Allman, D. *et al.* Thymopoiesis independent of common lymphoid progenitors. *Nat. Immunol.* **4**, 168–174 (2003).
6. Benz, C. & Bleul, C.C. A multipotent precursor in the thymus maps to the branching point of the T versus B lineage decision. *J. Exp. Med.* **202**, 21–31 (2005).
7. Bhandoola, A., von Boehmer, H., Petrie, H.T. & Zuniga-Pflucker, J.C. Commitment and developmental potential of extrathymic and intrathymic T cell precursors: plenty to choose from. *Immunity* **26**, 678–689 (2007).
8. Wada, H. *et al.* Adult T-cell progenitors retain myeloid potential. *Nature* **452**, 768–772 (2008).
9. Bell, J.J. & Bhandoola, A. The earliest thymic progenitors for T cells possess myeloid lineage potential. *Nature* **452**, 764–767 (2008).
10. Desanti, G.E. *et al.* Clonal analysis reveals uniformity in the molecular profile and lineage potential of CCR9^{+} and CCR9^{-} thymus-settling progenitors. *J. Immunol.* **186**, 5227–5235 10.4049/jimmunol.1002686 (2011).
11. Masuda, K. *et al.* Thymic anlage is colonized by progenitors restricted to T, NK, and dendritic cell lineages. *J. Immunol.* **174**, 2525–2532 (2005).
12. Kondo, M., Weissman, I.L. & Akashi, K. Identification of clonogenic common lymphoid progenitors in mouse bone marrow. *Cell* **91**, 661–672 (1997).
13. Adolfsson, J. *et al.* Identification of Flt3^{+} lympho-myeloid stem cells lacking erythro-megakaryocytic potential a revised road map for adult blood lineage commitment. *Cell* **121**, 295–306 (2005).
14. Orkin, S.H. & Zon, L.I. Hematopoiesis: an evolving paradigm for stem cell biology. *Cell* **132**, 631–644 (2008).
15. Luc, S., Buza-Vidas, N. & Jacobsen, S.E. Delineating the cellular pathways of hematopoietic lineage commitment. *Semin. Immunol.* **20**, 213–220 (2008).
16. Doulatov, S. *et al.* Revised map of the human progenitor hierarchy shows the origin of macrophages and dendritic cells in early lymphoid development. *Nat. Immunol.* **11**, 585–593 (2010).
17. Goardon, N. *et al.* Coexistence of LMPP-like and GMP-like leukemia stem cells in acute myeloid leukemia. *Cancer Cell* **19**, 138–152 (2011).
18. Taub, D.D. & Longo, D.L. Insights into thymic aging and regeneration. *Immunol. Rev.* **205**, 72–93 (2005).
19. Ceredig, R., Bosco, N. & Rolink, A.G. The B lineage potential of thymus settling progenitors is critically dependent on mouse age. *Eur. J. Immunol.* **37**, 830–837 (2007).
20. Sambandam, A. *et al.* Notch signaling controls the generation and differentiation of early T lineage progenitors. *Nat. Immunol.* **6**, 663–670 (2005).
21. Radtke, F. *et al.* Deficient T cell fate specification in mice with an induced inactivation of Notch1. *Immunity* **10**, 547–558 (1999).
22. Feyerabend, T.B. *et al.* Deletion of Notch1 converts pro-T cells to dendritic cells and promotes thymic B cells by cell-extrinsic and cell-intrinsic mechanisms. *Immunity* **30**, 67–79 (2009).
23. Hobeika, E. *et al.* Testing gene function early in the B cell lineage in mb1-cre mice. *Proc. Natl. Acad. Sci. USA* **103**, 13789–13794 (2006).
24. Srinivas, S. *et al.* Cre reporter strains produced by targeted insertion of EYFP and ECFP into the ROSA26 locus. *BMC Dev. Biol.* **1**, 4 (2001).
25. Campbell, K.J. *et al.* Elevated Mcl-1 perturbs lymphopoiesis, promotes transformation of hematopoietic stem/progenitor cells, and enhances drug resistance. *Blood* **116**, 3197–3207 (2010).
26. Kiel, M.J. *et al.* SLAM family receptors distinguish hematopoietic stem and progenitor cells and reveal endothelial niches for stem cells. *Cell* **121**, 1109–1121 (2005).
27. Balazs, A.B., Fabian, A.J., Esmon, C.T. & Mulligan, R.C. Endothelial protein C receptor (CD201) explicitly identifies hematopoietic stem cells in murine bone marrow. *Blood* **107**, 2317–2321 (2006).
28. Solar, G.P. *et al.* Role of c-mpl in early hematopoiesis. *Blood* **92**, 4–10 (1998).
29. Igarashi, H., Gregory, S.C., Yokota, T., Sakaguchi, N. & Kincade, P.W. Transcription from the RAG1 locus marks the earliest lymphocyte progenitors in bone marrow. *Immunity* **17**, 117–130 (2002).
30. Zlotoff, D.A. *et al.* CCR7 and CCR9 together recruit hematopoietic progenitors to the adult thymus. *Blood* **115**, 1897–1905 (2010).
31. Krueger, A., Willenzon, S., Lyszkiewicz, M., Kremmer, E. & Forster, R. CC chemokine receptor (CCR) 7 and 9 double-deficient hematopoietic progenitors are severely impaired in seeding the adult thymus. *Blood* **115**, 1906–1912 (2010).
32. Luc, S. *et al.* Downregulation of Mpl marks the transition to lymphoid-primed multipotent progenitors with gradual loss of granulocyte-monocyte potential. *Blood* **111**, 3424–3434 (2008).
33. Godfrey, D.I., Kennedy, J., Suda, T. & Zlotnik, A. A developmental pathway involving four phenotypically and functionally distinct subsets of CD3^{-}CD4^{-}CD8^{-} triple-negative adult mouse thymocytes defined by CD44 and CD25 expression. *J. Immunol.* **150**, 4244–4252 (1993).
34. Mansson, R. *et al.* Molecular evidence for hierarchical transcriptional lineage priming in fetal and adult stem cells and multipotent progenitors. *Immunity* **26**, 407–419 (2007).
35. Ehrlich, L.I., Serwold, T. & Weissman, I.L. In vitro assays misrepresent in vivo lineage potentials of murine lymphoid progenitors. *Blood* **117**, 2618–2624 (2011).
36. Inlay, M.A. *et al.* Ly6d marks the earliest stage of B-cell specification and identifies the branchpoint between B-cell and T-cell development. *Genes Dev.* **23**, 2376–2381 (2009).
37. Pronk, C.J.H. *et al.* Elucidation of the phenotypic, functional, and molecular topography of a myeloerythroid progenitor cell hierarchy. *Cell Stem Cell* **1**, 428–442 (2007).
38. David-Fung, E.S. *et al.* Transcription factor expression dynamics of early T-lymphocyte specification and commitment. *Dev. Biol.* **325**, 444–467 (2009).
39. Wendorff, A.A. *et al.* Hes1 is a critical but context-dependent mediator of canonical Notch signaling in lymphocyte development and transformation. *Immunity* **33**, 671–684 (2010).
40. Petrie, H.T. & Kincade, P.W. Many roads, one destination for T cell progenitors. *J. Exp. Med.* **202**, 11–13 (2005).
41. Chi, A.W. *et al.* Identification of Flt3CD150 myeloid progenitors in adult mouse bone marrow that harbor T lymphoid developmental potential. *Blood* **118**, 2723–2732 (2011).
42. Schlenner, S.M. *et al.* Fate mapping reveals separate origins of T cells and myeloid lineages in the thymus. *Immunity* **32**, 426–436 (2010).
43. Coustan-Smith, E. *et al.* Early T-cell precursor leukaemia: a subtype of very high-risk acute lymphoblastic leukaemia. *Lancet Oncol.* **10**, 147–156 (2009).
44. Metzler, M. *et al.* A conditional model of MLL-AF4 B-cell tumourigenesis using invertor technology. *Oncogene* **25**, 3093–3103 (2006).